Science Bulletin 68 (2023) 3048–3054

Contents lists available at ScienceDirect

Science Bulletin

journal homepage: www.elsevier.com/locate/scib

Article

Fragmentation of continental subduction is ending the Himalayan orogeny

Xiaofeng Liang [a,*], Yang Chu [a], Bo Wan [a], Ling Chen [a,b], Lin Chen [a], Eric Sandvol [c], Stephen P. Grand [d], Yibing Li [a], Minling Wang [e], Xiaobo Tian [a], Yun Chen [a,b], Tao Xu [a], Yang Li [a], Wei-Qiang Ji [a]

[a] State Key Laboratory of Lithospheric Evolution, Institute of Geology and Geophysics, Chinese Academy of Sciences (CAS), Beijing 100029, China
[b] CAS Center for Excellence in Deep Earth Science, Guangzhou 510640, China
[c] Department of Geological Sciences, University of Missouri, Columbia MO 65211, USA
[d] Department of Geological Sciences, University of Texas at Austin, Austin TX 78712, USA
[e] College of Earth Sciences, Guilin University of Technology, Guilin 541004, China

ARTICLE INFO

Article history:
Received 29 May 2023
Received in revised form 27 September 2023
Accepted 28 September 2023
Available online 27 October 2023

Keywords:
Tibetan Plateau
Seismic tomography
Continental collision
Slab fragmentation
Slab pull

ABSTRACT

After two continents collide, plate convergence and orogenesis are sustained because subducted continental lithosphere continues pulling the surface plate. It remains controversial how, why, and when continental plate convergence and collision slow down and eventually cease. We use an unprecedented data coverage and present a regional-scale seismic tomographic image of the mantle structure beneath the Tibetan Plateau. In the mantle transition zone, we identify multiple high-velocity anomalies and interpret them as detached pieces of the Indian continental slab. Facilitated by internal heterogeneity of the continental lithosphere, piecewise slab detachments could reduce the slab pull force, resulting in the Miocene slowdown of the India-Eurasia convergence and coeval diachronous potassic volcanism in southern Tibet. We propose that slab detachment is a mechanism that eventually will lead to the end of the Indo-Eurasian continental collision and the Himalayan orogeny.

1. Introduction

Global tomographic images show that oceanic lithosphere subducts deep into the mantle [1]. The negative buoyancy of slabs drives continuous subduction, which in turn drives plate movements and recycles lithospheric material into the deep mantle. Continent subduction after ocean closure results in significantly decreased plate convergence and extensive shortening of continents. After continental collision, subduction can persist as evidenced by ultra-high-pressure metamorphic rock records of deeply subducted continental crust [2] and seismic images of subducting continental slabs [3,4], but at some point subduction stops. It is not clear why and how continental subduction stops, though the process is critical for understanding plate tectonics and the formation of super-continents [5]. The collision of India and Eurasia produced the Himalayan orogen and Tibetan Plateau, the highest mountain chains and plateau on Earth, and also provides a classic example of continent–continent collision that preserves ultra-high-pressure rocks [6] and is currently in convergence [7]. Whether and how long the collision and uplift will continue remain unclear although the region has been extensively studied from the surface to deep mantle [8–14].

Here, we provide a new high-resolution tomographic image of the upper mantle beneath the India-Eurasia collision zone using a recently collected and compiled dataset. This dataset includes all available temporary seismic networks that have operated over the past twenty years and offers the possibility of significantly improving the resolution of deep structure imaging compared to previous studies. Our new image shows separated fast velocity anomalies in the mantle transition zone (MTZ) that we interpret as fragments of subducted continental slab. We further discuss the connection of these detachments to ultra-potassic magmatism in southern Tibet [15,16] and the slowing-down of the convergence rate between the Indian and Eurasian plates [17–20] since the late-Miocene that may eventually lead to the cessation of the Himalayan orogeny.

2. Seismic tomography results

We used a total of 773 seismic stations that cover a region from the southern Himalaya in Nepal to central Tibet, with especially dense coverage in central and southern Tibet (Fig. 1). A

* Corresponding author.
E-mail address: liangxf@mail.iggcas.ac.cn (X. Liang).

https://doi.org/10.1016/j.scib.2023.10.017
2095-9273/

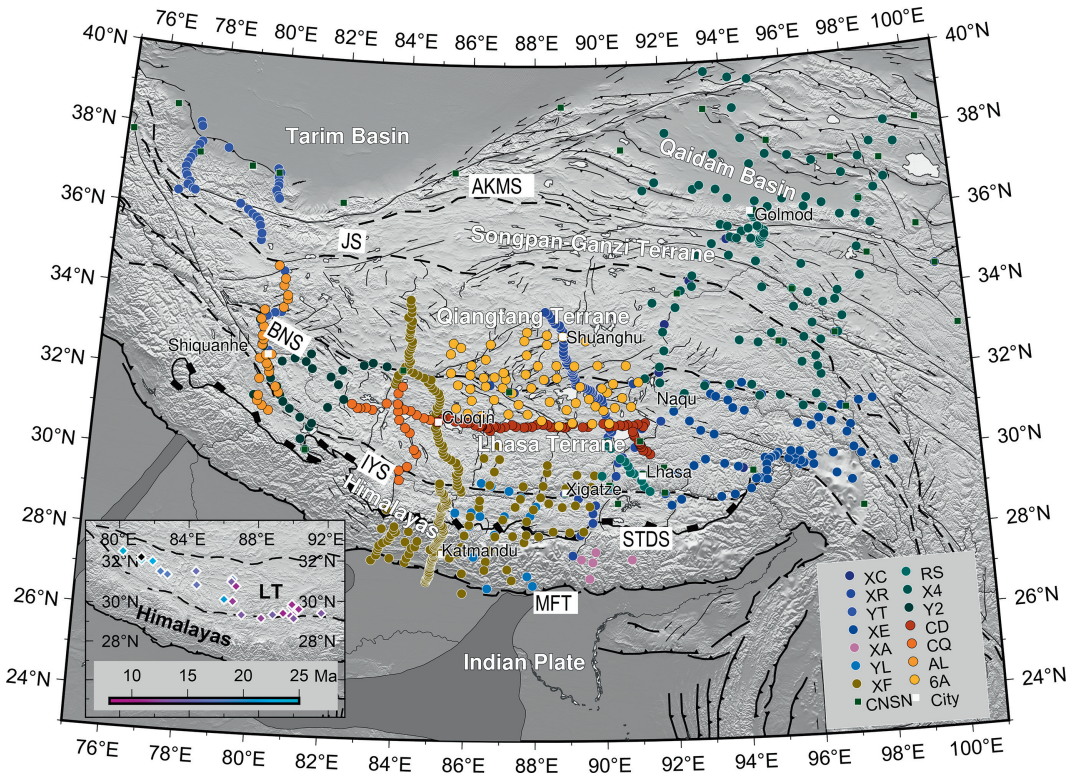

Fig. 1. Seismic station locations and tectonic map. Grey-shaded areas on the Indian plate are basement ridges [21]. Structures from the HimaTibetMap dataset [22] include MFT: Main Frontal Thrust, STDS: Southern Tibetan Detachment System, IYS: Indus-Yarlung Suture, BNS: Bangong-Nujiang Suture, JS: Jinsha Suture, and AKMS: Ayimaqin-Kunlun-Mutztagh Suture. The network codes for different seismic arrays are XC: PASSCAL91, XR: INDEPTH, YT: West Kunlun, XE: Namcha Barwa, XA: Buhtan, YL: HIMNT, XF: Hi-CLIMB, RS: RISE, X4: ASCENT, Y2: West Tibet, CD: Tibet-31 N, CQ: West Cuoqin, AL: TW-80, 6A: SANDWICH, and CNSN: Chinese National Seismic Network. Locations of ultrapotassic rocks in southern Tibet with emplacement ages [15,16] are shown as color-coded diamonds in the inset. LT: Lhasa Terrane. The details for the different arrays are discussed in Supplementary materials (online).

finite-frequency seismic tomographic method (see Supplementary materials and Figs. S1–S3 online) was used to invert for the relative upper mantle P- and S-wave velocity (*Vp* and *Vs*) structure beneath the region. Relative travel time residuals were measured using the multi-channel cross-correlation method [23] for asynchronous temporary seismic datasets with the long-lived permanent IC.LSA station as the reference. We also considered relative sensitivity kernels by removing an average sensitivity function for each seismic event to accommodate the potential effects of different deployments (see Supplementary materials online). A recent global *Vp* model DETOX-P3 [24] and a *Vs* model SEISGLOB2 [25] were used as the initial model for the *Vp* and *Vs* inversions (Figs. S4–S6 online), respectively. After the inversion we obtained comprehensive 3D *Vp* and *Vs* images of the upper mantle beneath southern and central Tibet (Fig. 2 and Figs. S7–S9 online) that provide insights into the geometry of the Indian continental lithosphere beneath the Tibetan Plateau. Since the major features of the tomographic images in the shallow mantle (Figs. S7 and S8 online) are similar to previous studies [26], suggesting a fragmented subducting Indian lithosphere [27,28] and heterogenous Tibetan lithosphere related to different amalgamated terranes and possible lithosphere delamination [12,29,30], we will focus on the MTZ portion of the model in this paper.

A prominent feature in the model is the presence of two isolated high-velocity anomalies (HV1 and HV2, Fig. 2) in the MTZ beneath the Himalayas. One is located at 80°–87°E with a width of 100–200 km near 28°N. The other is located at 90°–94°E with a width of 100–200 km at around 28.5°N. They both extend from about 390 to 660 km depth to the south of the Indus-Yarlung suture (IYS). Based on the spatial distribution of these anomalies and the post-collisional convergence distance between the Indian and Eurasian plates, we interpret these bodies as early-stage detachments of the northern edge of the Indian continental lithosphere.

Another prominent high-velocity anomaly (HV3) is observed in the MTZ with a ~40° north-dipping trend beneath the Lhasa terrane. This anomaly can be found from ~86° to 92°E, although it is not clear whether it is vertically continuous. This high-velocity anomaly steepens and deepens from west to east, as it reaches ~450 km depth at ~30.5°N along 86.5°E (Fig. 2 and Fig. S8 online, section A–A′), then ~500 km depth at ~31°N along 88.5°E (Fig. 2 and Fig. S8 online, section B-B′) and finally ~660 km at ~32°N along 91°E (Fig. 2 and Fig. S8 online, section C–C′). There exists a lateral gap in HV3 from ~88° to 92°E at about 200 km depth, showing a transition of a thin high-velocity anomaly to a low-velocity gap from west to east (Fig. 2 and Fig. S8 online, sections A–A′, B–B′, and C–C′, "necking"). This high-velocity body has been interpreted in prior studies as the subducting Indian continental lithosphere [26]. Its east–west variation indicates possible ongoing detachment of slab, which would make it a younger version of the HV1 and HV2 bodies to the south. It might be closely related to the proposed slab tearing of the subducting Indian lithosphere [27,28,31]. One more high-velocity anomaly (HV4) is observed beneath western Tibet near the BNS and extending to the northern edge of the plateau between 80° and 86°E. HV4 may be another piece of the detaching Indian continental lithosphere. Resolution tests (Figs. S10–S12 online) show the ability of the data set to recover velocity anomalies on this scale. Customized resolution tests show that the four isolated high velocity anomalies are well resolved (Fig. S10e, f online). It is worth noting that there is also

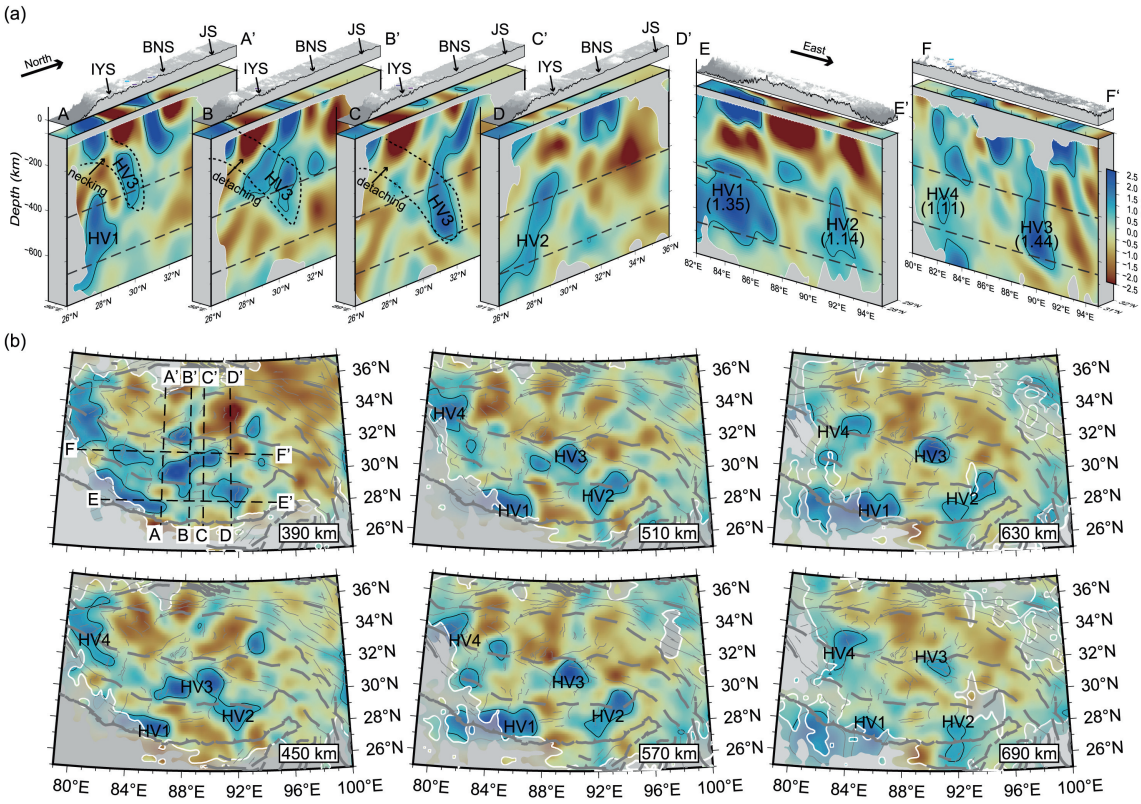

Fig. 2. P-wave velocity tomographic images along different cross-sections (a) and at different depths in the mantle transition zone (b). The location of the cross-sections is indicated in the upper-left plot of (b). Four high velocity anomalies (HVs) are labeled as HV1, HV2, HV3, and HV4 with their average magnitude on E–E′ and F–F′ cross-sections. The thin black lines show the contours of 0.8% *Vp* perturbation. The thick dashed gray lines are the suture zones labeled in Fig. 1. The images are clipped according to the 75% cross-correlation coefficient of checkerboard tests and the thick-white lines show the 80% contours. The areas between coefficients of 75% and 80% are shaded out. The dashed lines on the cross-sections highlight the proposed subducting Indian continental lithosphere. The acronyms of sutures as same as Fig. 1 are shown on top of each cross-section.

an apparent well-resolved gap between HV3 and HV4 in the MTZ (Fig. 2). The other seismic studies also revealed HVs in the MTZ for central and western Tibet [32–42] (Fig. S13 online).

3. Break-off of subducted Indian lithosphere

Determining the origin of HV1 and HV2 can potentially yield important constraints on the evolution of the India-Eurasian collisional process. Molnar et al. [43] have suggested there is convective removal of a thickened Tibetan lithosphere, primarily beneath northern Tibet, where the uppermost mantle is seismically slow and highly attenuated [27,29,44–47] and Cenozoic potassic volcanic rocks are widely exposed [15]. This raises the possibility that HV1 and HV2 represent two portions of delaminated thickened Qiangtang lithosphere. However, the horizontal distance of about 500 km between the HV anomalies and northern Tibet argues against this scenario. If a delamination/foundering of the thickened lithosphere did take place beneath the Qiangtang terrane, the isolated HV anomalies would have appeared further north in the MTZ. Since the resolution in the MTZ of our tomographic model is limited beneath the Qiangtang and Songpan-Ganzi terranes, we cannot exclude the possibility that existing HV anomalies in the MTZ beneath northern Tibet are masked by a strong low velocity zone in the shallow mantle (Fig. S11 online). Nonetheless, the observation of HV1 and HV2 beneath southern Tibet requires processes other than lithospheric delamination in northern Tibet.

Assuming the four HV anomalies in the MTZ originated from the Indian continental lithosphere, we can use the spatial relationships of HV1, HV2, HV3, and HV4 to recover the geometry of the India-Eurasian plate boundary before the Miocene. HV3 and HV4 may still be attached to the subducting Indian continental lithosphere, so recovering their original locations is straightforward. Assuming that detached slabs sink vertically, the current horizontal locations of HV1 and HV2 should be where they were detached from the subducting Indian continental lithosphere. The complicated interactions between the subducted/detached slabs and the MTZ [48] are not considered in this study. The initial northern edge of the Indian continent is thus reconstructed by attaching HV1, HV2, HV3, and HV4 to the northern edge of the current Indian plate (Fig. S14, Supplementary materials online), suggesting that the subducted Indian passive margin had a limited width (~900 km) if all HV anomalies in the MTZ are continental lithosphere. This is in agreement with the paleo-geographic reconstruction, indicating a limited size of the Indian passive continental margin [49].

The present-day locations of the four isolated high velocity anomalies in the MTZ imply diachronous detachments of the Indian continental lithosphere. HV1 and HV2 are south of HV3 and HV4, beneath the Himalayas and the proposed subducting Indian continental lithosphere. We propose that these lithospheric fragments (HV1 and HV2) have been detached from the subducted Indian continental lithosphere and were overridden by the later subducting Indian continental lithosphere, HV3 and HV4. The relative velocity perturbations of the HV anomalies (Fig. 2) establish a temporal sequence of their sinking into the MTZ. The simplest

interpretation is that the longer an anomaly stays in the MTZ, the lower the magnitude of the velocity perturbation as the temperature difference diffuses. This implies an early to late order of detachment of HV2, HV1, and HV3 (Supplementary materials online). We do not further discuss HV4, because it consists of several smaller anomalies in the MTZ, possibly a result of poor resolution due to sparse station coverage in northwestern Tibet.

The interpretation that the HVs are the result of diachronous detachment of the Indian continental lithosphere is consistent with the tectono-magmatic evolution of the India-Eurasian collisional zone [50–52]. Tempo-spatially scattered across southern Tibet, Late Oligocene-Miocene (25–8 Ma) ultrapotassic-potassic magmatic rocks (Fig. 3a) are originated from either delamination of the lower part of the southern Tibetan lithospheric mantle, or detachment/break-off of the subducting Indian continental lithosphere [15,56]. The ultrapotassic volcanics appear to systematically migrate eastward at a rate of ~6.5 cm/a (Fig. 4a) which is consistent with the modelled propagation rate of a slab tear [58], but is not consistent with the eruptive style resulting from lithospheric delamination in the central Andes [59]. In the central Andean Plateau where delamination is very likely observed, we see eruptions with larger volumes, shorter time frames, and the presence of widespread crustal melting (e.g., ignimbrites). These observations lend further support to a slow detachment of the subducting Indian continental lithosphere [51] rather than a fast delamination of the southern Tibetan lithosphere. Relative to the east–west trending detached fragment HV1 (Fig. 1), the NWW (N288°) trending track of ultrapotassic volcanism requires an approximately 2 cm/a northward shortening of the overlying Tibetan lithosphere, in agreement with the GPS-based shortening rate [60], which suggest a similar shortening rate of the Tibetan lithosphere since the Miocene [19]. It is noteworthy that the eastern Lhasa terrane lacks ultrapotassic magmatism but outcrops an adakitic intrusion [15,56] during the same time period, possibly related to the detachment of HV2. The ultrapotassic volcanics may have been fully eroded in the east after their emplacement due to the higher exhumation rate of the eastern Himalayas [61]. The Southern Tibetan Detachment System (STDS) is a set of orogen-parallel normal-sense faults and shear zones that have been traced along the entire Himalayan orogen [13]. It became inactive following an eastward trend [51,53] similar to that of the ultrapotassic volcanism (Fig. 3a). This would be consistent with a post-break-off extensional-compressional inversion along the passive margin.

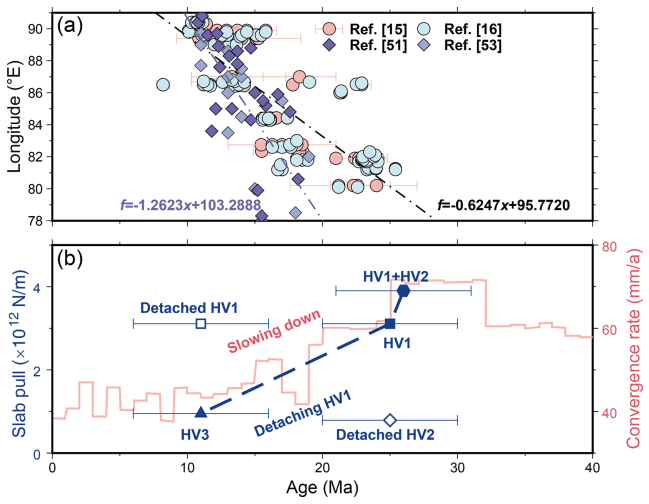

Fig. 3. Comparison among different geological observations with our proposed slab pull evolution. (a) The eastward younging trends and corresponding least-square fitting of both the emplacement ages of ultrapotassic volcanism (circles) [15,16] and cessation times of the Southern Tibet Detachment System (diamonds) [51,53] in southern Tibet. Only Ar–Ar ages are used for their indications of latest ductile deformation. (b) Our proposed evolution of slab pull from the detached lithospheric slices. At the beginning, both HV1 and HV2 contributed to the slab pull, as HV1 + HV2 (hexagon); then HV2 was detached (without explicit geological records for its detaching process), and its slab pull (diamond) diminished; and then the slow detachment of HV1 occurred, and so did the removal of the corresponding slab pull (squares); finally, HV3 subducted into the upper mantle and exerted slab pull (triangle). Dashed lines show the potential evolution path of slab pull. Blue horizontal bars on slab pull show a 5 Ma error estimated from the emplacement age of ultrapotassic volcanics. The convergence rate (pink line) between the Indian and Eurasian plates [54,55] is also plotted for comparison. A set of convergence rate between the Indian and Eurasian plates from previous studies can be found in Fig. S16 (online) for comparison.

4. Diminishing slab pull

Adopting temperature–velocity derivatives from phase equilibrium modeling using Perple_X [62], we estimated temperature-induced density anomalies from the imaged velocity perturbations, and thus quantified the subducting Indian continental lithosphere-exerted slab pull force (Figs. S15-S18 and Supplementary materials online). We calculated the potential slab pull from HV1 and HV2 as ~$(3.90 \pm 2.41) \times 10^{12}$ N/m (Supplementary materials online), which is two to four times [63] or about one and half [18] of the estimated ridge push from the Indian ridge. The mantle suction/-dragging applied to the base of the lithosphere may not necessarily be as large as ~2×10^{12}–3×10^{12} N/m [63] due to the slab pull from the subducted Indian continental lithosphere. But the asthenospheric flow would potentially contribute to the plate convergence between the Indian and Eurasian plates [64,65]. Moreover, metamorphic phase transitions involving the eclogitization of the lower crust [66] and the transformation from coesite to stishovite in the felsic crust [67] provided an additional negative buoyancy to the subducted continental lithosphere. The slab pull force driving the Indian plate ultimately helped to build the high plateau, through the accumulation of gravitational potential energy [19,63]. When a piece of the Indian continental lithosphere detached, the corresponding slab pull would diminish and slow the India-Eurasia convergence (Fig. 3b and Fig. S19 online). The detached piece of the slab might have been deflected and thus stagnated within the MTZ, due to the viscosity and density jumps across the spinel–perovskite phase boundary [68].

The different sizes of the detached lithosphere slices (Supplementary materials online) are consistent with lithospheric partitioning and suggest they may have detached along preexisting weak zones in the Indian continental lithosphere. The Indian plate consists of several tectonic units assembled along pre-Neoproterozoic orogens to form Eastern Gondwana [57]. The northern edge of the Indian continent was a passive continental margin with thinned lithosphere before entering the trench [14,69]. The basement rocks of the Himalaya are proposed to be involved in the Neoproterozoic Pan-African orogeny [70]. These ancient orogens were rheologically weaker than the Precambrian cratonic keels and thus could facilitate the detachment process. The viscosity of the weak zones in the Indian continental lithosphere has been estimated to be ~8×10^{22} Pa s (Supplementary materials online), about one order of magnitude weaker than the average continental lithosphere [71]. Consequently, the lower yield strength of these pre-existing lithospheric weak zones and the negative buoyancy of the deeper portion of the subducted Indian continental lithosphere, combined with the increasing positive buoyancy of the impinging Indian lithosphere, drive the lithospheric break-off (Fig. S15 online). Several basement ridges beneath the foreland Ganges basin may exemplify these weak zones [21] (Fig. 1). The increasing positive buoyancy of the Indian

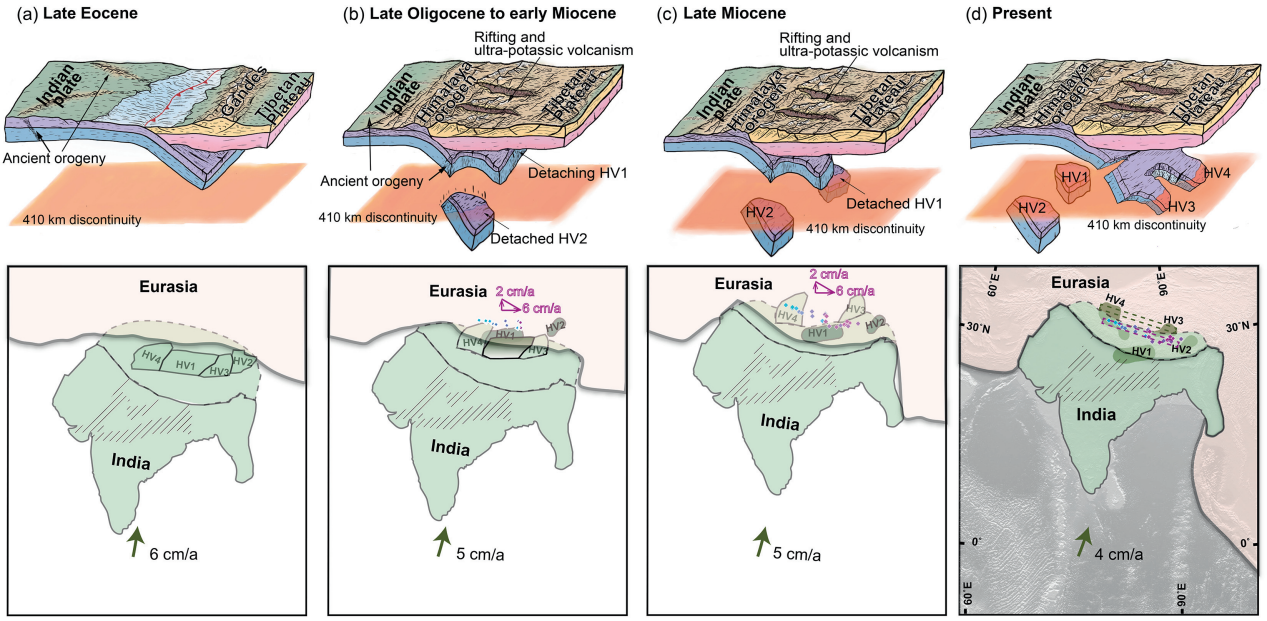

Fig. 4. Schematic cartoons showing the evolution of the subducted northern edge of the Indian continent. (a) Subduction of the reconstructed northern part of the Indian plate during the late Eocene. (b) A piece of subducted Indian lithosphere detached and then sank into the MTZ as HV2, and another piece of subducted lithosphere HV1 continued exerting slab pull. The detachment of the slab patch has initiated the rifting process in the southern Tibet shown as the two brown strips in the cartoon. (c) The subducted Indian lithosphere HV1 was detached and sank into the MTZ (dark green blocks in the lower panel). Its detaching process was accompanied by ultrapotassic volcanism and continuation of the rifting process. The purple arrows show the eastward migration velocity of the ultrapotassic volcanism and northward shortening rate of the overlying Tibetan lithosphere. (d) Present distribution of the HV anomalies in the MTZ. The dashed purple rectangle shows the NW-SE elongated distribution of ultrapotassic volcanism. The dashed dark green rectangle shows the spatial extent of the subducted Indian continental lithosphere in the MTZ as represented by HV3 and HV4. Gray shaded areas in the Indian continent are basement ridges and other Proterozoic tectonic belts [57]. Relative positions of the Indian and Eurasian plates are from Molnar and Stock [17].

plate is due to the difference in chemical composition of mature cratonic lithosphere [72]. Our density estimation for three mantle compositions suggests that intact cratonic lithospheric mantle is too buoyant to sink into the asthenospheric mantle, even considering its much lower temperature (Supplementary materials and Fig. S18 online). We propose that the slab pull will decrease and finally vanish as the entire subducted slab breaks off, at which time the two continents will become one coherent plate. The Indian craton may block the collision zone, and provide a docking force at the surface that facilitates the final break-off of the subducted slab.

Detachment of subducted lithosphere will likely induce an asthenospheric upwelling, overriding plate extension, enhanced compression and surface uplift for the collision zone [73], and ultimately a slow-down of convergence. A number of geological observations are consistent with this model. The altitude of the Himalaya rose from ~2.3 km at the start of the Miocene [74] to > 5.0 km by 15 Ma [75], which broadly coincided with a 40% slowdown in the convergence rate from 20 to 11 Ma [17,19,54]. Most of the north–south trending rifts in southern Tibet also began in the Miocene [16]. Both the cessation of the STDS and the emplacement of ultrapotassic rocks show a consistent eastward younging trend starting at the beginning of the Miocene [51] (Fig. 3a). The peak tectonic exhumation of the Greater Himalaya occurred at about 23 Ma [76]. Finally, the detachments successfully explain spatio-temporal patterns in magmatism, sudden elevation rise of the Himalaya, crustal extension in southern Tibet, a major change in global atmospheric circulation, and transition in denudation and metamorphism as a single deep Earth process [50].

We have identified four isolated high velocity anomalies within the MTZ beneath southern Tibet. Combining these observations with the four-dimensional distribution of ultrapotassic volcanism in southern Tibet, we propose a piecewise break-off of the subducted Indian lithosphere along lithospheric weak zones (Fig. 4). It is suggested that continental subduction will end when the entire subducted slab breaks off with the subsequent elimination of the slab pull force, which eventually will suture the two continents. Our result suggests limited recycling of continental lithospheric material into the mantle through continental subduction, which explains the long-term preservation of continents since the Archean.

Conflict of interest

The authors declare that they have no conflict of interest.

Acknowledgments

This work was supported by the National Natural Science Foundation of China (91855207, 42074067, and 42030308) and the Strategic Priority Research Program (B) of the Chinese Academy of Sciences (XDB18000000) and the Youth Innovation Promotion Association of the Chinese Academy of Sciences (2017093). Seismic Array Laboratory, Institute of Geology and Geophysics, Chinese Academy of Sciences (IGGCAS) provided instruments and maintenance services for field experiments CD, CQ, AL, and 6A. We also acknowledge the Data Management Center, Incorporated Research Institutions for Seismology (current Seismological Facility for the Advancement of Geosicence) and the X4, XC, XE, XF, XR, YL, YT, Y2, and RS experiments for making seismic data available. Our manuscript has benefited from discussions with Chuan-Zhou Liu, Shi-Hu Li, Xiao-Chi Liu, Yi Chen from IGGCAS, Zhi-Chao Liu from Sun Yat-sen University, Matthew J. Kohn at Boise State University and James Connolly at Eidgenössische Technische Hochschule Zürich and brainstorm in Coffice 442, IGGCAS. Min Chen at Michigan State University and Zewei Wang at Southern University of

Science and Technology shared their Tibetan velocity model. Sofia-Katerina Kufner at Karlsruhe Institute of Technology helped in figure preparation.

Author contributions

Xiaofeng Liang, Yang Chu, Bo Wan, Ling Chen, Eric A. Sandvol, Stephen P. Grand, Xiaobo Tian, and Yun Chen developed the conceptualization of the project. Xiaofeng Liang, Xiaobo Tian, Yun Chen, and Tao Xu collected the seismic data used in the study. Xiaofeng Liang, Eric A. Sandvol, Stephen P. Grand, Ling Chen, Xiaobo Tian, Yun Chen, Tao Xu, Yibing Li, Lin Chen, Yang Li, and Wei-Qiang Ji conducted the data analysis and calculation. Xiaofeng Liang and Yang Chu prepared all the figures. All authors extensively discussed the results and jointly developed implications. Xiaofeng Liang, Yang Chu, Bo Wan, Ling Chen, Eric A. Sandvol, Stephen P. Grand, Lin Chen, Yibing Li, and Yang Li wrote the original manuscript. All authors participated in finalizing the manuscript.

Appendix A. Supplementary materials

Supplementary materials to this article can be found online at https://doi.org/10.1016/j.scib.2023.10.017.

References

[1] van der Hilst RD, Widiyantoro S, Engdahl ER. Evidence for deep mantle circulation from global tomography. Nature 1997;386:578–84.
[2] Chopin C. Ultrahigh-pressure metamorphism: tracing continental crust into the mantle. Earth Planet Sci Lett 2003;212:1–14.
[3] Levander A, Bezada MJ, Niu F, et al. Subduction-driven recycling of continental margin lithosphere. Nature 2014;515:253–6.
[4] Zhao L, Malusà MG, Yuan H, et al. Evidence for a serpentinized plate interface favouring continental subduction. Nat Commun 2020;11:2171.
[5] Gutierrez-Alonso G, Fernandez-Suarez J, Weil AB, et al. Self-subduction of the pangaean global plate. Nat Geosci 2008;1:549–53.
[6] Wang J-M, Lanari P, Wu F-Y, et al. First evidence of eclogites overprinted by ultrahigh temperature metamorphism in Everest East, Himalaya: implications for collisional tectonics on early Earth. Earth Planet Sci Lett 2021;558:116760.
[7] Wang M, Shen Z-K. Present-day crustal deformation of continental China derived from GPS and its tectonic implications. J Geophys Res 2020;125: e2019JB018774.
[8] Replumaz A, Capitanio FA, Guillot S, et al. The coupling of Indian subduction and Asian continental tectonics. Gondwana Res 2014;26:608–26.
[9] Parsons AJ, Hosseini K, Palin R, et al. Geological, geophysical and plate kinematic constraints for models of the India-Asia collision and the post-Triassic central Tethys oceans. Earth Sci Rev 2020;208:103084.
[10] Li C, van der Hilst RD, Meltzer AS, et al. Subduction of the Indian lithosphere beneath the Tibetan Plateau and Burma. Earth Planet Sci Lett 2008;274:157–68.
[11] van der Meer DG, van Hinsbergen DJJ, Spakman W. Atlas of the underworld: slab remnants in the mantle, their sinking history, and a new outlook on lower mantle viscosity. Tectonophysics 2018;723:309–448.
[12] Chen M, Niu F, Tromp J, et al. Lithospheric foundering and underthrusting imaged beneath Tibet. Nat Commun 2017;8:15659.
[13] Yin A. Cenozoic tectonic evolution of the Himalayan orogen as constrained by along-strike variation of structural geometry, exhumation history, and foreland sedimentation. Earth Sci Rev 2006;76:1–131.
[14] Capitanio FA, Morra G, Goes S, et al. India-Asia convergence driven by the subduction of the greater Indian continent. Nat Geosci 2010;3:136–9.
[15] Guo Z, Wilson M. Late oligocene–early miocene transformation of postcollisional magmatism in Tibet. Geology 2019;47:776–80.
[16] Bian S, Gong J, Zuza AV, et al. Late pliocene onset of the Cona rift, eastern Himalaya, confirms eastward propagation of extension in Himalayan-Tibetan orogen. Earth Planet Sci Lett 2020;544:116383.
[17] Molnar P, Stock JM. Slowing of India's convergence with Eurasia since 20 Ma and its implications for Tibetan mantle dynamics. Tectonics 2009;28:1–11.
[18] Copley A, Avouac J-P, Royer J-Y. India-Asia collision and the Cenozoic slowdown of the Indian plate: implications for the forces driving plate motions. J Geophys Res 2010;115:B03410.
[19] Clark MK. Continental collision slowing due to viscous mantle lithosphere rather than topography. Nature 2012;483:74–7.
[20] Iaffaldano G, Bodin T, Sambridge M. Slow-downs and speed-ups of India-Eurasia convergence since: data-noise, uncertainties and dynamic implications. Earth Planet Sci Lett 2013;367:146–56.
[21] Godin L, La Roche RS, Waffle L, et al. Influence of inherited Indian basement faults on the evolution of the Himalayan orogen. Geol Soc Spec Publ 2018;481:251–76.
[22] Styron R, Taylor M, Okoronkwo K. Database of active structures from the Indo-Asian collision. EOS Trans AGU 2010;91:181–2.
[23] VanDecar JC, Crosson RS. Determination of teleseismic relative phase arrival times using multi-channel cross-correlation and least squares. Bull Seismol Soc Am 1990;80:150–69.
[24] Hosseini K, Sigloch K, Tsekhmistrenko M, et al. Global mantle structure from multifrequency tomography using P, PP and P-diffracted waves. Geophys J Int 2020;220:96–141.
[25] Durand S, Debayle E, Ricard Y, et al. Confirmation of a change in the global shear velocity pattern at around 1000 km depth. Geophys J Int 2017;211:1628–39.
[26] Liang X, Chen Y, Tian X, et al. 3D imaging of subducting and fragmenting Indian continental lithosphere beneath southern and central Tibet using body-wave finite-frequency tomography. Earth Planet Sci Lett 2016;443:162–75.
[27] Liang X, Sandvol E, Chen YJ, et al. A complex Tibetan upper mantle: a fragmented Indian slab and no south-verging subduction of Eurasian lithosphere. Earth Planet Sci Lett 2012;333-334:101–11.
[28] Li J, Song X. Tearing of Indian mantle lithosphere from high-resolution seismic images and its implications for lithosphere coupling in southern Tibet. Proc Natl Acad Sci USA 2018;115:8296–300.
[29] Wittlinger G, Masson F, Poupinet G, et al. Seismic tomography of northern Tibet and Kunlun: evidence for crustal blocks and mantle velocity contrasts. Earth Planet Sci Lett 1996;139:263–79.
[30] Tilmann F, Ni J, INDEPTH Seismic Team. Seismic imaging of the downwelling Indian lithosphere beneath central Tibet. Science 2003;300:1424–7.
[31] Chen Y, Li W, Yuan X, et al. Tearing of the Indian lithospheric slab beneath southern Tibet revealed by SKS-wave splitting measurements. Earth Planet Sci Lett 2015;413:13–24.
[32] Chu R, Zhu L, Ding Z. Upper-mantle velocity structures beneath the Tibetan Plateau and surrounding areas inferred from triplicated P waveforms. Earth Planet Phys 2019;3:444–58.
[33] Tseng T-L, Chen W-P. Discordant contrasts of P- and S-wave speeds across the 660-km discontinuity beneath Tibet: a case for hydrous remnant of subcontinental lithosphere. Earth Planet Sci Lett 2008;268:450–62.
[34] Li G, Bai L, Zhang H, et al. Velocity anomalies around the mantle transition zone beneath the Qiangtang terrane, central Tibetan Plateau from triplicated P waveforms. Earth Space Sci 2022;9:e2021EA002060.
[35] Feng J, Yao H, Chen L, et al. Massive lithospheric delamination in southeastern Tibet facilitating continental extrusion. Natl Sci Rev 2022;9:nwab174.
[36] Duan Y, Tian X, Liang X, et al. Subduction of the Indian slab into the mantle transition zone revealed by receiver functions. Tectonophysics 2017;702:61–9.
[37] Saikia D, Kumar MR, Singh A. Palaeoslab and plume signatures in the mantle transition zone beneath eastern Himalaya and adjoining regions. Geophys J Int 2020;221:468–77.
[38] Wu Y, Bao X, Zhang B, et al. Seismic evidence for stepwise lithospheric delamination beneath the Tibetan Plateau. Geophys Res Lett 2022;49: e2022GL098528.
[39] Xu M, Huang Z, Wang L, et al. Lateral variation of the mantle transition zone beneath the Tibetan Plateau: insight into thermal processes during Indian-Asian collision. Phys Earth Planet Inter 2020;301:106452.
[40] Yue H, Chen YJ, Sandvol E, et al. Lithospheric and upper mantle structure of the northeastern Tibetan Plateau. J Geophys Res 2012;117:B05307.
[41] Zhang R, Wu Y, Gao Z, et al. Upper mantle discontinuity structure beneath eastern and southeastern Tibet: new constraints on the Tengchong intraplate volcano and signatures of detached lithosphere under the western Yangtze Craton. J Geophys Res 2017;122:1367–80.
[42] Bai Y, Yuan X, He Y, et al. Mantle transition zone structure beneath Myanmar and its geodynamic implications. Geochem Geophys Geosyst 2020;21: e2020GC009262.
[43] Molnar P, England P, Martinod J. Mantle dynamics, uplift of the Tibetan Plateau, and the Indian monsoon. Rev Geophys 1993;31:357–96.
[44] Ni J, Barazangi M. High-frequency seismic wave propagation beneath the Indian Shield, Himalayan Arc, Tibetan Plateau and surrounding regions: high uppermost mantle velocities and efficient Sn propagation beneath Tibet. Geophys J Int 1983;72:665–89.
[45] Barron J, Priestley K. Observations of frequency-dependent Sn propagation in northern Tibet. Geophys J Int 2009;179:475–88.
[46] Hearn TM, Ni JF, Wang H, et al. Depth-dependent P_n velocities and configuration of Indian and Asian lithosphere beneath the Tibetan Plateau. Geophys J Int 2019;217:179–89.
[47] Zhao L, Zhao M, Lu G. Upper mantle seismic anisotropy beneath a convergent boundary: SKS waveform modeling in central Tibet. Sci China Earth Sci 2014;57:759–76.
[48] Li Z-H, Gerya T, Connolly JAD. Variability of subducting slab morphologies in the mantle transition zone: insight from petrological-thermomechanical modeling. Earth Sci Rev 2019;196:102874.
[49] Ali JR, Aitchison JC. Greater India. Earth Sci Rev 2005;72:169–88.
[50] Ding L, Kapp P, Cai F, et al. Timing and mechanisms of Tibetan Plateau uplift. Nat Rev Earth Environ 2022;3:652–67.
[51] Webb AAG, Guo H, Clift PD, et al. The Himalaya in 3D: slab dynamics controlled mountain building and monsoon intensification. Lithosphere 2017;9:637–51.
[52] van Hinsbergen DJJ. Indian plate paleogeography, subduction and horizontal underthrusting below Tibet: paradoxes, controversies and opportunities. Natl Sci Rev 2022;9:nwac074.

[53] Liu Z-C, Wu F-Y, Qiu Z-L, et al. Leucogranite geochronological constraints on the termination of the south Tibetan detachment in eastern Himalaya. Tectonophysics 2017;721:106–22.
[54] van Hinsbergen DJJ, Steinberger B, Doubrovine PV, et al. Acceleration and deceleration of India-Asia convergence since the cretaceous: roles of mantle plumes and continental collision. J Geophys Res 2011;116:B06101.
[55] Zahirovic S, Müller RD, Seton M, et al. Insights on the kinematics of the India-Eurasia collision from global geodynamic models. Geochem Geophys Geosyst 2012;13:Q04W11.
[56] Chung S-L, Chu M-F, Zhang Y, et al. Tibetan tectonic evolution inferred from spatial and temporal variations in post-collisional magmatism. Earth Sci Rev 2005;68:173–96.
[57] Wang W, Cawood PA, Pandit MK, et al. No collision between eastern and western Gondwana at their northern extent. Geology 2019;47:308–12.
[58] von Tscharner M, Schmalholz SM, Duretz T. Three-dimensional necking during viscous slab detachment. Geophys Res Lett 2014;41:4194–200.
[59] Kay RW, Kay SM. Delamination and delamination magmatism. Tectonophysics 1993;219:177–89.
[60] Zheng G, Wang H, Wright TJ, et al. Crustal deformation in the India-Eurasia collision zone from 25 years of GPS measurements. J Geophys Res 2017;122:9290–312.
[61] Cao W, Yang J, Zuza AV, et al. Crustal tilting and differential exhumation of gangdese batholith in southern Tibet revealed by bedrock pressures. Earth Planet Sci Lett 2020;543:116347.
[62] Connolly JAD. Computation of phase equilibria by linear programming: a tool for geodynamic modeling and its application to subduction zone decarbonation. Earth Planet Sci Lett 2005;236:524–41.
[63] Ghosh A, Holt WE, Flesch LM, et al. Gravitational potential energy of the Tibetan Plateau and the forces driving the Indian plate. Geology 2006;34:321–4.
[64] Parsons AJ, Sigloch K, Hosseini K. Australian plate subduction is responsible for northward motion of the India-Asia collision zone and ~1000 km lateral migration of the Indian slab. Geophys Res Lett 2021;48:e2021GL094904.
[65] Zhu W, Ding L, Ji Y, et al. Subduction evolution controlled Himalayan orogenesis: implications from 3-D subduction modeling. Appl Sci 2022;12:7413.
[66] Shi D, Klemperer SL, Shi J, et al. Localized foundering of Indian lower crust in the India-Tibet collision zone. Proc Natl Acad Sci USA 2020;117:24742–7.
[67] Wang Y, Zhang L, Li Z-H. Metamorphic densification can account for the missing felsic crust of the greater Indian continent. Commun Earth Environ 2022;3:166.
[68] Zhong S, Gurnis M. Mantle convection with plates and mobile, faulted plate margins. Science 1995;267:838–43.
[69] Hu X, Garzanti E, Wang J, et al. The timing of India-Asia collision onset—facts, theories, controversies. Earth Sci Rev 2016;160:264–99.
[70] DeCelles PG, Gehrels GE, Quade J, et al. Tectonic implications of U-Pb zircon ages of the Himalayan orogenic belt in Nepal. Science 2000;288:497–9.
[71] Kohlstedt DL, Evans B, Mackwell SJ. Strength of the lithosphere: constraints imposed by laboratory experiments. J Geophys Res 1995;100:17587–602.
[72] Djomani YHP, O'Reilly SY, Griffin WL, et al. The density structure of subcontinental lithosphere through time. Earth Planet Sci Lett 2001;184:605–21.
[73] Husson L, Bernet M, Guillot S, et al. Dynamic ups and downs of the Himalaya. Geology 2014;42:839–42.
[74] Ding L, Spicer RA, Yang J, et al. Quantifying the rise of the Himalaya orogen and implications for the south Asian monsoon. Geology 2017;45:215–8.
[75] Gébelin A, Mulch A, Teyssier C, et al. The miocene elevation of Mount Everest. Geology 2013;41:799–802.
[76] Kohn MJ, Corrie SL. Preserved Zr-temperatures and U-Pb ages in high-grade metamorphic titanite: evidence for a static hot channel in the Himalayan orogen. Earth Planet Sci Lett 2011;311:136–43.

Xiaofeng Liang is an associate research professor at the Institute of Geology and Geophysics, Chinese Academy of Sciences (IGGCAS). His research interest focuses on conducting seismicity analysis and seismic imaging to explore the crust and upper mantle structures in collisional and subduction orogenic regions. He also has a keen interest in researching material recycling processes that occur within the Earth and on other celestial bodies.